Securing food under adverse climate and socioeconomic scenarios in Jiangsu Province, China

Critical role of human adaptation under change

Lyu, Haoyang; Dong, Zengchuan; Pande, Saket

DOI
10.1016/j.jhydrol.2021.126344

Publication date
2021

Document Version
Final published version

Published in
Journal of Hydrology

Journal of Hydrology 598 (2021) 126344

Contents lists available at ScienceDirect

Journal of Hydrology

journal homepage: www.elsevier.com/locate/jhydrol

Research papers

Securing food under adverse climate and socioeconomic scenarios in Jiangsu Province, China: Critical role of human adaptation under change

Haoyang Lyu [a,b], Zengchuan Dong [a,*], Saket Pande [b]

[a] College of Hydrology and Water Resources, Hohai University, Nanjing, China
[b] Department of Water Management, Delft University of Technology, Delft, Netherlands

ARTICLE INFO

This manuscript was handled by Nandita Basu, Editor-in-Chief, with the assistance of Marc F. Muller, Associate Editor

Keywords:
Climate change
Food security
Scenario analysis
Water and nutrient use efficiencies
Trade-off between human labor and machinery in agriculture

ABSTRACT

Food security is important for human well-being worldwide. However, changing climate, population growth and shrinking land resources are threatening food security in many regions of the world. Jiangsu Province, China, is one such region. It is a major food-producing region of the country but is witnessing rapid population growth and urbanization that is putting pressure on agricultural water and land resources and threatening food security of the region.

This paper interprets the nexus between regional water availability and food security in Jiangsu Province under different climate change and socio-economic scenarios of population growth and land resource availability. Climate change scenarios are generated based on historical data and Global Climate Model (GCM) products. Socio-economic scenarios are generated based on population growth and crop planted area projections.

The uptake of water and nutrients are considered as two dominant biophysical processes of crop growth and food production. Complementing it is human agency, including human labor, irrigation and land-preparation machinery, which are the factors behind water and nutrient use efficiencies of crops grown. Two dominant crops are considered, rice and wheat, that contribute to 61.4% of total crops produced in the province.

Results show that adaptation by human agency is necessary to ensure that food supply meets at least the demand of the province under all climate change and socio-economic scenarios. Under relatively favorable scenarios, labor could replace land-preparing machinery since the level of food production can be easily maintained with abundant water and land availability. Mechanization in agricultural production significantly increases food production under unfavorable conditions, since it improves water and nutrient use efficiencies and leads to higher crop yields. This demonstrates that human agency plays an important role in securing food under stressful scenarios of drier climate, population growth, and contraction of agricultural lands.

1. Introduction

Maintaining sufficient food supply is key to a healthy population and social stability (Springmann et al., 2016; Kaiser, 2011). This can either be realized through trade or through high and stable level of food produced locally. The latter is especially important under changing climate and evolving socio-economic conditions (Turral et al., 2011), such as rapid population growth (McCarthy et al., 2018), and shrinking agricultural lands (Hou et al., 2019; Qiu et al., 2020). This is because trade will likely be disrupted more often, offering less reliable means of securing food for local population (Cardwell, 2014).

Under changing climate, local food production is expected to be affected by changing water availability and impact food security and agricultural employment (Hertel and Rosch, 2010; Rosemberg, 2010; Siwar et al., 2013). Food security, i.e. when food supply of a region is at least able to meet its own demand, is affected directly by such changing agro-ecological conditions and crop yields, as well as indirectly by inequitable distribution of incomes (Schmidhuber and Tubiello, 2007). Changing socio-economic conditions (Garibaldi and Pérez-Méndez, 2019), such as shrinking agricultural land resources for food crops, are also expected to reduce overall food production (van Vliet et al., 2017; Wang, 2019). This exasperates food insecurity with rising demand for food due to population growth (Avery et al., 2019; Mondal and Sanaul, 2019).

Jiangsu Province, China, is one such region that exemplifies the pressures on food security. As one of the major regions of crop

* Corresponding author.
E-mail address: zcdong@hhu.edu.cn (Z. Dong).

https://doi.org/10.1016/j.jhydrol.2021.126344
Received 19 January 2021; Received in revised form 2 April 2021; Accepted 13 April 2021
Available online 17 April 2021

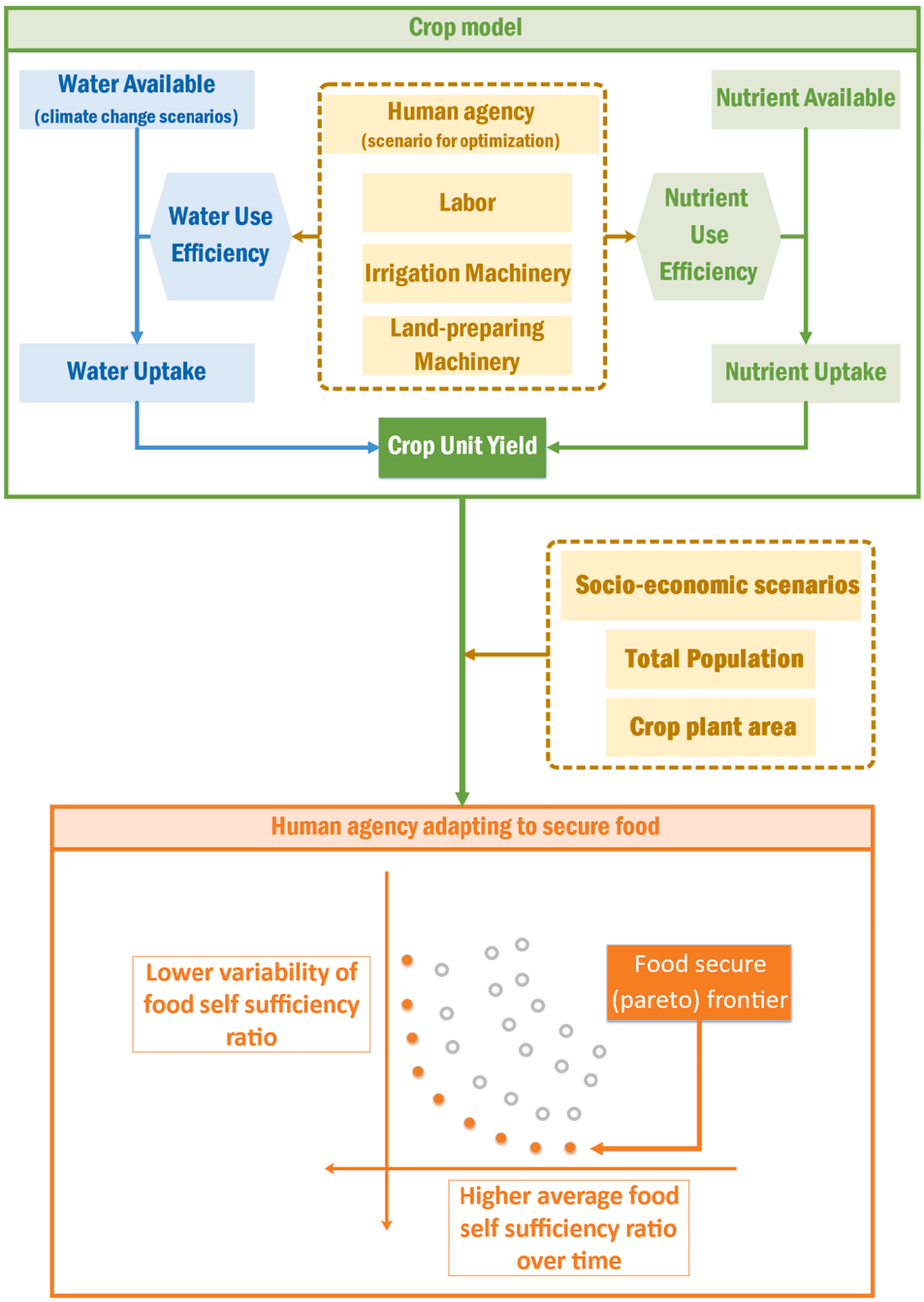

Fig. 1. Illustration of the overall methodology. FSR stands for Food Sufficiency Ratio, which is the ratio of food demand and food supply.

production in China (Gu and Guo, 2011), the province produces 37 million tons of food crops (BSC, 2019) and supports the enormous food demand of the country. It is also one of the regions which is under water stress (Li and Li, 2012; Xu et al., 2011), and witnessing land and population growth pressures (Zhang et al., 2004; Qian et al., 2008; Zhu and Ou, 2020). With agricultural land shrinking in the process of urbanization, people are shifting from rural agriculture to modern industries, leading to rural to urban migration (Lyu et al., 2019). The province is likely to face food insecurity in the future and adaptation strategies are urgently needed (Xu and Ding, 2015).

Often not enough adaptation to bio-physical impacts, high-cost of measures, short-term merit but long-term negative adaptations, and lack of feasible adaptive strategies hinder adequate response to climate and socioeconomic changes (Warner and Geest, 2013). This highlights the need to unravel possible means to adapt under diverse future scenarios and secure sufficient food (Challinor et al., 2010), which move away from more expensive hard interventions such as supply oriented measures to soft interventions. Examples of the latter include how water and land resources are governed and used in crop production (Medeiros and Sivapalan, 2020; Li and Sivapalan, 2020; Kakinuma et al., 2014).

This paper uniquely views humans as agents of change that improve water and nutrient use efficiencies, and inquires to what extent food security can be ensured for Jiangsu Province. Since most food crops are farmed, labor is an indispensable part of such human agency (Achille et al., 2015). The agency also includes machineries, for irrigation and land-preparation, which improves the efficiency of water and nutrients uptakes for food crop production (Febrina et al., 2013; Ma et al., 2020; Huang et al., 2018).

The human agency can adapt crop production to changing conditions and secure food (Crane et al., 2011; Olesen et al., 2011; Leisnham et al.,

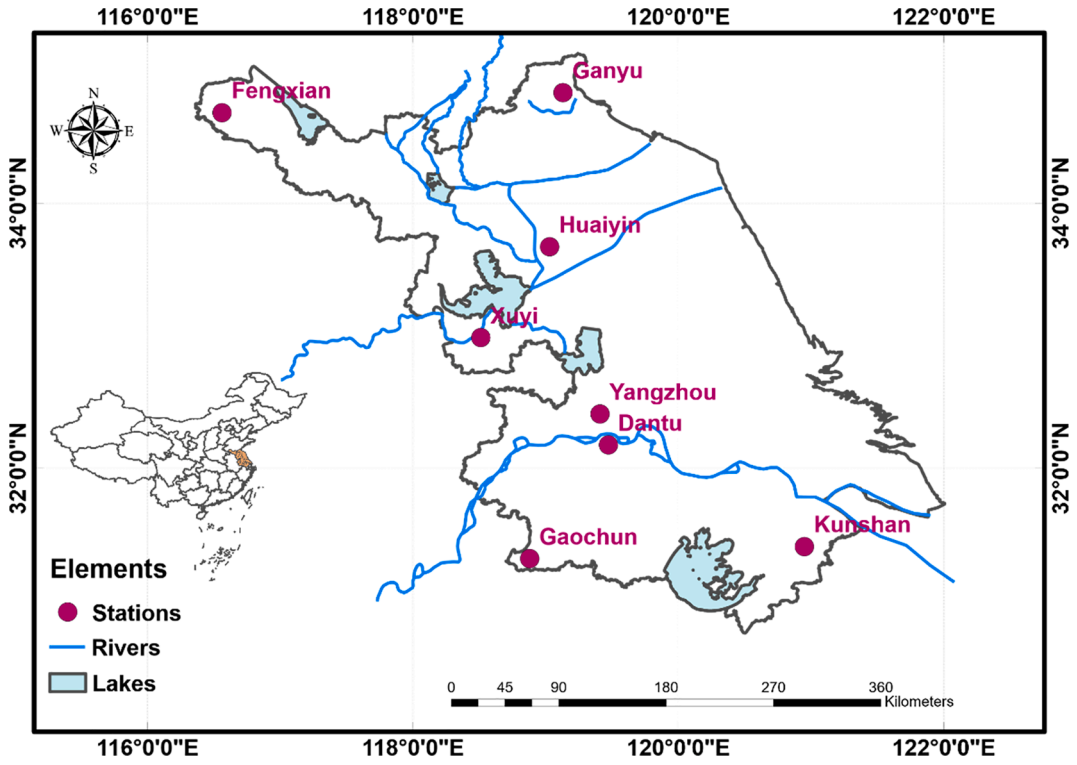

Fig. 2. Jiangsu Province, China. Also shown are the stations that are used in the study.

2013; Preston et al., 2015; Gomez-Zavaglia et al., 2020). However, no studies yet exist that have modelled human agency in context of crop production and assessed the effects of its adaptation to changing environment on food security. The aim of the paper is to assess the extent to which food security can be ensured by adapting human agency under changing conditions of water and land availability in Jiangsu Province.

The paper is organized into five sections. Section 2 describes the methodology used for generating climate change and socio-economic scenarios, modeling crop production, evaluating food security and maximizing it by adapting human agency, together with the main data sources used. Section 3 presents the results of "optimized" food security under different climate and socio-economic scenarios. Section 4 first discusses the improvements in crop water and nutrient use efficiencies that are brought about by adapting human agency. It then discusses the trade-offs between labor and machinery employed to optimize food security under different climate change and socio-economic scenarios. Section 5 then summarizes the main conclusions.

2. Methods and materials

Fig. 1 illustrates the overall methodology. A crop model which combines bio-physical mechanisms with human agency (Lyu et al., 2020) is applied. Climate change brought about by greenhouse gas emissions is assumed to effect crop yields due to changes in precipitation. The human agency, including labor, irrigation machinery power and land-preparing machinery power per unit area, determines the water and nutrient use efficiencies during crop growth.

The socio-economic conditions are assumed to be dominated by population growth and food crop plant area and affect crop production and the ratio of food supply to food demand, i.e. food self-sufficiency rate – a key indicator of food security.

The human agency adapts to changing climate and socio-economic conditions by improving the water and nutrient use efficiencies of food crops so that higher yields are achieved. The food self-sufficiency rate within Jiangsu Province is then determined as the ratio of food supply and food demanded for given population and planted area scenarios. Here food supply is the product of yield and planted area and food demand is determined by the dietary demand of the population of the province.

Finally, it is assumed that the objective of adaptation by human agency is to jointly maximize the magnitude and stability (i.e. lower variance) of food self-sufficiency rate (FSR) for a given climate change and socioeconomic scenario over the next 30 years till 2050. The human agency adapts in order to identify non-dominated sets of higher and stabler (lower variance) FSRs. Here by non-dominated sets it is meant that there are no other sets that dominate this set in terms of either having higher or stabler FSR.

2.1. Study area

As shown in Fig. 2, Jiangsu Province is located in the southeastern coast of China. The province is in a transition zone between subtropical and warm temperate climate, with annual precipitation around 1000 mm/year. Three of the main rivers of China run through it: Yi-Shu-Si, Huaihe and Yangzi (including the Taihu Lake river network). Benefiting from its abundant river systems and water resources, Jiangsu is one of the main exporters of food crops to other provinces in China (Li et al., 2009). It is able to supply food not only for its own residents, but also to other provinces across the country.

There are eight crop-monitoring stations providing crop locations and related information of the growing seasons. Six stations for wheat: Fengxian, Ganyu, Xuyi, Huaiyin, Yangzhou, Kunshan and three stations for rice: Ganyu, Dantu, Gaochun, are considered.

2.2. Stochastic climate scenario generation

Representative Concentration Pathways (RCPs) (IPCC, 2019) have been applied as emission scenarios for climate backgrounds to generate regional precipitation and temperature time series with uncertainty (Lobell et al., 2006). Regional precipitation time series have been produced with a multi-model climate generator called Simgen (Greene et al., 2012, 2015; Greene, 2012). The Simgen climate generator

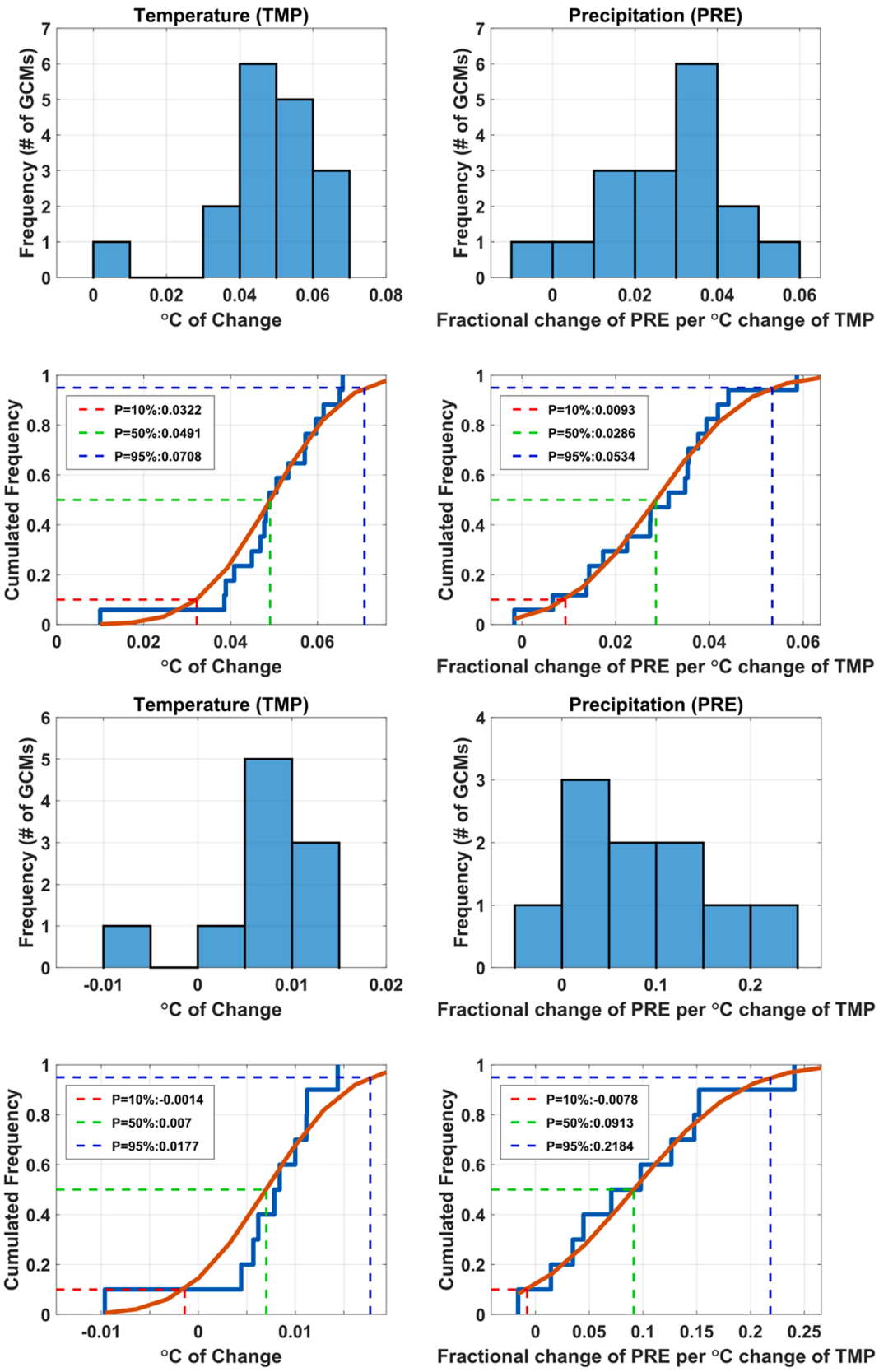

Fig. 3. a Frequency distribution representing GCM related uncertainty and selection of percentile models under RCP 8.5. b Frequency distribution representing GCM related uncertainty and selection of models at 10, 50 and 90 percentiles under RCP 2.6.

incorporates nonlinear climate change trends, inferred using an ensemble of global climate models from the Coupled Model Intercomparison Project (CMIP5) (Taylor et al., 2012; Meehl and Hibbard, 2007; Hibbard et al., 2007; Hurrell et al., 2011).

Under a given RCP condition, Simgen first uses a selected number of Global Climate Models (GCMs) to simulate historical precipitation data at the stations within the study area (as shown in Fig. 2) and evaluates the performance of each GCM based on its correlation with the historical precipitation time series (Greene et al., 2012; Eyring, 2013; Aloysius et al., 2016). GCMs with correlation coefficients higher than 0.50 are selected for generating climate scenario time series for future time steps. The frequency distributions of temperature change (°C) and fractional change of precipitation with per °C change of temperature, together with the cumulative frequency distribution function (CDF) of the selected GCMs for RCPs 8.5 and 2.6 are shown in Fig. 3a, b, for the study area.

A combination of a selected GCM (corresponding to a percentile on the frequency distribution) with a RCP used by Simgen then produces corresponding precipitation and temperature time series with stochastic effects. Here, 100 runs each of 2×3 combinations of two RCPs (2.6, 8.5) and three GCM percentiles (10%, 50%, 95%) are used to generate climate change scenarios. For more details on Simgen, readers are referred to Greene (2012).

RCP2.6 represents a pathway where the radiation forcing reaches to about 3 W/m^2 before 2100 and then declines. The corresponding greenhouse gas emission concentration path (Emission Concentration Pathway, ECP) assumes constant emissions after 2100. RCP8.5 represents a pathway in which the radiation forcing reaches greater than 8.5 W/m^2 and continues to rise after 2100. The corresponding ECP assumes constant greenhouse gas emission after 2100 and constant greenhouse gas concentration after year 2250.

Precipitation time series have been generated for the six wheat crop stations and three rice crop stations (see Fig. 2). For each combination of RCP and GCM percentile, the generated climate scenarios have four dimensions: $P(t)_{i,j,k}$, where t is the time step (50 years from 2001 to 2050 in total, with climate scenarios applied since 2018), i denotes crop type (1 for wheat and 2 for rice), j represents crop-monitoring station ($j \in [1,6]$ for wheat, $j \in [1,3]$ for rice), k indexes a stochastic run of Simgen with given RCP and GCM percentile (100 runs in total)

2.3. Generation of options for adaptation by human agency

Labor (capita), irrigation machinery (power) and land-preparing machinery (power) per unit area are treated as human agency. It improves the efficiencies of water and nutrient uptake, thereby improving crop yields.

In order to generate realistic options for adaptation by human agency, appropriate data generating processes that describe temporal evolution of human agency are first identified. These are based on growth rate time series from 2002 to 2017 of labor force, g_L, irrigation machinery power, g_{MI} and land-preparing machinery power, g_{ML}.

Autoregressive Integrated Moving Average model (Kotu and Deshpande, 2018), ARIMA(1,0,0) is applied to the time series of g_L, g_{MI} and g_{ML}, as it is found to be most appropriate model of the past time series. Being ARIMA(1,0,0), the lag coefficients of the models, i.e., τ_L, τ_{MI}, and τ_{ML}, for respective time series are sufficient to describe the time series.

In order to stochastically simulate the time series, 2000 tuples of ARIMA coefficients τ_L, τ_{MI}, and τ_{ML} within the range of $[-0.9999, 0.9999]$ are randomly sampled for a given climate scenario. The generated coefficient tuples are then expressed as $[\tau_{L,r}, \tau_{MI,r}, \tau_{ML,r}]$, $r \in [1, 2000]$. With 2000 samples of coefficient tuples, time series of g_L, g_{MI} and g_{ML} are stochastically generated and 2000 human agency time series of human labor force, irrigation machinery power and land-preparing machinery power per area are thus obtained.

2.4. Crop production simulation

As shown in Fig. 1, a crop production model is used that combines both bio-physical factors and human agency in simulating crop yields. Lyu et al., (2020) have demonstrated its utility in simulating wheat and rice production in Jiangsu Province, China.

The crop production model treats Normalized Difference Vegetation Index (NDVI) as resulting from the joint effect of water and nutrient uptakes on plant greenness. Therefore, the effect of water uptake (represented by transpiration T) on NDVI is first filtered out and the remaining variance of NDVI is then assumed to approximate the effect of uptake of nutrients N. The yield-uptake relationship is then defined in the form of a production function $Y = \lambda {x_W}^{\alpha} {x_N}^{\beta}$, where Y is crop yield, x_W is water uptake given by $\eta_W P$, x_N is nutrient uptake given by $\eta_N F$, α and β are corresponding elasticities and λ is a scaling factor. This production function represents the biophysical responses of crop yields to water and nutrient uptakes (Lyu et al., 2020). The parameters (λ, α, β) therefore do not assess economic or technological aspects of human agency. The human agency determines the water and nutrient use efficiencies, η_W and η_N respectively, that translate available water P and applied nutrients F to water and nutrient uptakes x_W and x_N respectively. The relationship between water or nutrient use efficiency and human agency is estimated based on the following equations:

$$\eta_W^j = \Lambda H^j + \delta^j + \epsilon_W$$

$$\eta_N^j = \Theta H^j + \theta^j + \epsilon_N \quad (1a,b)$$

Here, j refers to a crop-monitoring station, H^j represent station-specific human activities but its effect on efficiencies, (Λ, Θ), are general across all the stations. Fixed station-specific effects are quantified by (δ^i, θ^i), and (ϵ_W, ϵ_N) represent the residuals accounting for the variances of efficiencies not explained by H.

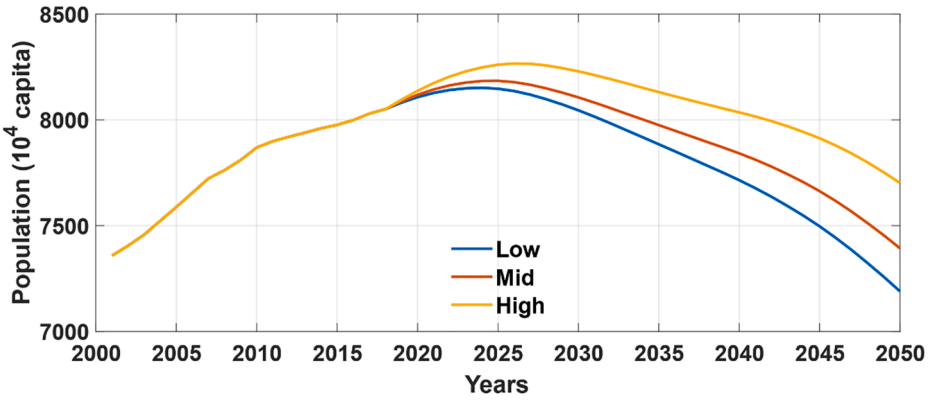

Fig. 4. Socio-economic scenario I: Population.

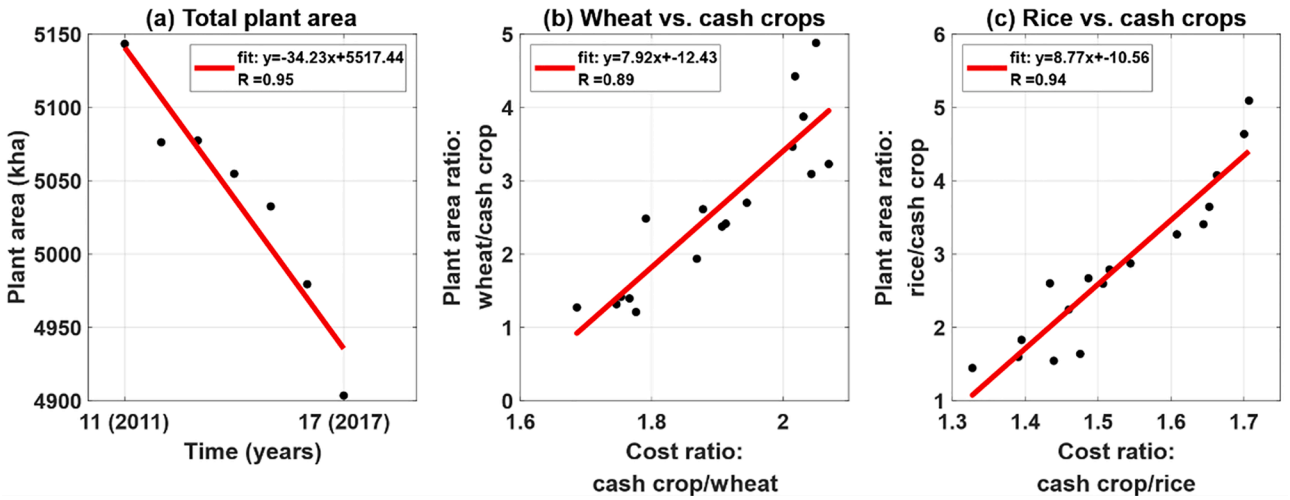

Fig. 5. Crop plant areas and calibration of forecasting models.

Human agency such as labor used in crop production L_C, irrigation machinery power M_I and land-preparing machinery power M_L per unit area are considered in the set of independent variables H. All combinations of joint and individual effects (such as $L_CM_IM_L$,L_CM_I, M_IM_L,L_CM_I, L_C,M_I andM_L) are first regressed and only those effects that were statistically significant are selected in the final model. In the calibration of Eq. 1, station specific observed values of η_W and η_N were calculated as $\eta_W = \frac{T}{P}$ and $\eta_N = \frac{N}{F}$, where T and P are transpiration and precipitation fluxes respectively integrated over the crop growing seasons, N is the nutrient proxy, and F is fertilizer use per area, which is the nutrient resource for croplands. See supplementary materials for the estimated parameters of the equations.

Climate change scenarios impose its effects on crop growth via precipitation P (Kawuma Menya, 2011; Kukal and Irmak, 2018; Makowski et al., 2020). The simulated crop yields (i.e., crop production per unit planted area) under each climate scenario (i.e., a combination of a RCP and a GCM percentile) q for either wheat or rice is represented by variable $Y(t)_{j,p,q,r}$, where t is time step (50 years from 2001 to 2050, with climate scenarios applied since 2018), j represents a crop-monitoring station ($j \in [1,6]$ for wheat, $j \in [1,3]$ for rice), r denotes human agency scenario ($r \in [1,2000]$), and p represents a stochastic run of Simgen under each climate scenario, $p \in [1,100]$.

2.5. Socio-economic scenarios

For a given level of crop yield as determined by the human agency factors under a climate change scenario, socio-economic conditions linked to population and plant area finally determine the level of food self-sufficiency within the study area.

As shown in Fig. 4, three scenarios of population (Low, Mid, High) have been simulated based on provincial population prediction datasets (Bureau of Statistics of Jiangsu, 2002, 2012) and the observed time series of population within the province (Bureau of Statistics of Jiangsu, 2019).

The crop plant area scenarios are based on the planted area dataset in the Statistical Yearbook of Jiangsu (Bureau of Statistics of Jiangsu, 2018) and the cost per unit area dataset in the China Rural Statistical Yearbook (National Bureau of Statistics, 2002~2018). Future crop planted area time series have been simulated based on relationships between two food crops (wheat, rice) and six cash crops (used as benchmark) since these crops compete over finite land area available and the decisions to grow which crops are affected by the costs of growing those crops (Chen et al., 2016; Zhao and Yan, 2019). It is assumed that farmers are cost minimizers. The farmers decide on how much area is allocated to food crops relative to cash crops based on minimizing costs (Chen, 2019; Mo et al., 2020). Corresponding efficiency conditions imply linear relationships between areas under food crops relative to cash crops and costs of cash crops relative to food crops.

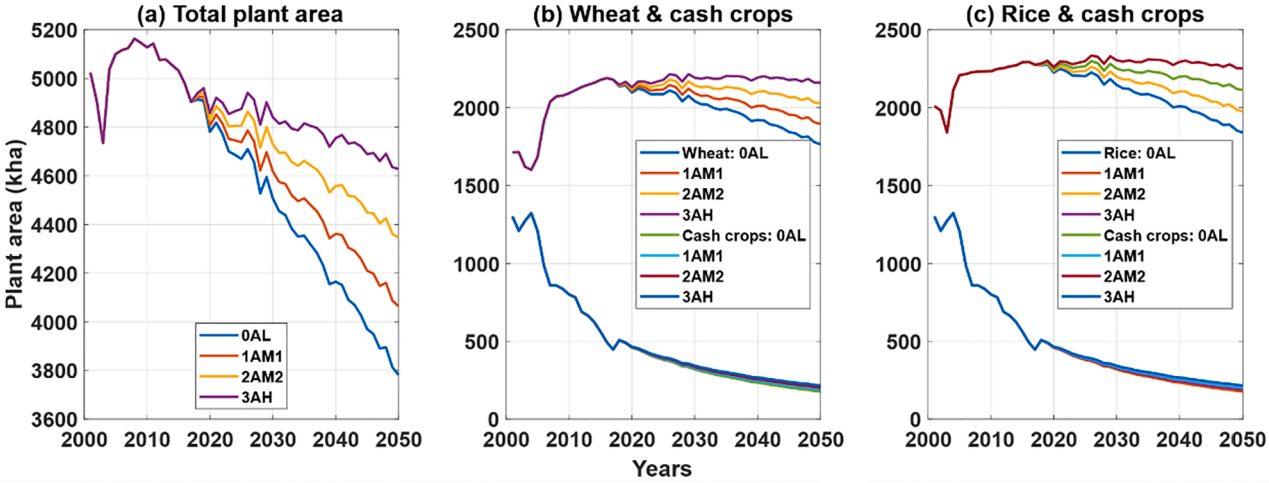

Fig. 6. Crop plant area scenarios.

Following steps outline the steps taken to unravel the linear relationships.

First the time series of the total planted areas of the eight selected crops are observed to vary linearly in time. A linear forecasting model ($R = 0.95$, p-value $< 10^{-3}$, as shown in Fig. 5a) is used to estimate past trend based on historical data from 2011 to 2018 and to generate trend-based scenarios of total planted area for the future.

The ratios of food crop planted areas with the six cash crops (C) planted areas are then estimated based on linear regressions, with the ratios of cash crop average cost per unit area with the food crops cost per unit area as the independent variables:

$$\frac{A_V}{A_C} = f_1\left(\frac{Y_C}{Y_V}\right)$$

$$\frac{A_R}{A_C} = f_2\left(\frac{Y_C}{Y_R}\right) \quad (2a,b)$$

where A_V and A_R are the planted areas of wheat (V) and rice (R) respectively, Y_V, Y_R and Y_C are the costs per unit areas of wheat, rice and cash crops respectively, and f_1 and f_2 are linear functions. Fig. 5b and 5c show the regression results for wheat ($R = 0.84$, p-value $<10^{-4}$) and for rice ($R = 0.92$, p-value $<10^{-7}$). It shows that the cash crops within the province have been gradually replaced by food crops because the cost per unit area of cash crops have been increasing relative to that of food crops. Finally, the slope of the trend line for total planted area, estimated based on historical data above, is used to generate scenarios for future areas planted under food crops.

According to the Statistical Yearbook of Jiangsu, in 2018 the area planted under wheat and rice in Jiangsu was 4618.68 kha (103 ha), whereas the area under the six cash crops was 274.93 kha (i.e., ~5% of area under food crops). This means that food crops have already dominated the cash crops in the province and may not significantly increase in the future. Therefore, the future scenarios of area under food crops only considered stable or declining trends, i.e., constant or negative slopes of the linear forecasting models for wheat and rice, for it to be realistic. Random errors were added based on the residuals between observed and linear model of the historic data.

Four scenarios from low to high slopes are created as shown in Fig. 6. The lowest slope scenario is based on the slope displayed in Fig. 5a, the other three use scaled slopes which are 75%, 50%, and 25% of the slope in the lowest slope scenario. As shown in Fig. 6, the four crop plant area scenarios, from low to high, were named as '0AL', '1AM1', '2AM2' and '3AH'. 'A' means 'Area', 'L', means 'Low', 'M' means 'Medium', and 'H' means 'High'.

2.6. Food security indicator: self-sufficiency ratio

Food self-sufficiency rate, Ψ, is defined as the ratio of food crop production to food crop demand of the province.

The food crop production per capita is calculated as follows:

$$Y(t)_{m,n,p,q,r} = \frac{\frac{A_V(t)_n}{6}\sum_{j=1}^{6} Y_V(t)_{j,p,q,r} * + \frac{A_R(t)_n}{3}\sum_{j=1}^{3} Y_R(t)_{j,p,q,r}}{\phi(t)_m} \quad (3)$$

where,

$Y(t)_{m,n,p,q,r}$ is the food crop production per capita at time step t, for human agency scenario r with precipitation time series p, (for each climate scenario q there are $k \in [1, 100]$ precipitation time series with stochastic effects of climate), under plant area scenario n and population scenario m.

$A_V(t)_n$ and $A_R(t)_n$ are the plant areas of wheat (V) and rice (R) at time t, under plant area scenario n.

$\phi(t)_m$ is the population at time step t, under population scenario m.

j represent the agricultural meteorological monitoring stations, for wheat $j \in [1,6]$, for rice $j \in [1,3]$. Note that the numerator of equation (3) is the sum of wheat and rice production levels averaged over the six and three corresponding stations respectively.

The calculation of self-sufficiency ratio $\Psi(t)_{m,n,p,q,r}$ is defined as.

$$\Psi(t)_{m,n,p,q,r} = \frac{Y(t)_{m,n,p,q,r}}{D} \quad (4)$$

where,

$Y(t)_{m,n,p,q,r}$ is the food crop production per capita.

D is the demand per capita for wheat and rice. The total food crop demand was assumed as 400 kg/capita (Wang et al., 2013). No shift in diet is considered that may lead to changes either in the total demand for food crops per capita or in the demand for wheat relative to rice. Considering that the total production of wheat and rice in 2018 accounted for about 88.7% of all food crops (BSC, 2019), a factor of 0.90 is used to estimate total D for wheat and rice as 360 kg/capita.

2.7. Food security

Under each of the six climate change scenarios (two RCPs and three GCM percentiles), 100 precipitation time series are stochastically generated. For each such generation, 2000 human agency options are applied that are randomly sampled according to the ARIMA model to obtain corresponding crop yields for rice and wheat. Then 12 socio-economic scenarios, i.e., three population scenarios and four crop planted area scenarios, are used to estimate the food sufficiency ratio within Jiangsu Province, China.

For a given climate scenario q, population scenario m, and crop planted area scenario n, a collection of food self-sufficiency rates $\Psi(t)_{m,n,p,q,r}$, are obtained. Note here that $r \in [1, 2000]$ denotes the human agency options, i.e., combination of labor, irrigation and land-preparing machinery power per unit area of cropland and $p \in [1, 100]$ denotes the 100 precipitation time series with stochastic effects under the given climate scenario q.

Simplifying $\Psi(t)_{m,n,p,q,r}$ to $\Psi(t)_{p,r}$, a two-dimensional food security indicator is estimated that considers the magnitude and variance of food sufficiency ratio over time.

In order to estimate the average magnitude of food sufficiency, average of food sufficiency ratio is first estimated over the 100 stochastic precipitation time series.

$$\overline{\Psi}(t)_r = \frac{1}{100}\sum_{p=1}^{100} \Psi(t)_{p,r} \quad (5)$$

The magnitude and variance of food self-sufficiency rate are then obtained by the equations below respectively,

$$\dot{\overline{\Psi}}_r = \frac{1}{50}\sum_{t=1}^{50} \overline{\Psi}(t)_r \quad (6a)$$

$$\sigma_{\overline{\Psi}_r} = \sqrt{\frac{1}{50-1}\sum_{t=1}^{50}\left|\overline{\Psi}(t)_r - \frac{1}{50}\sum_{t=1}^{50}\overline{\Psi}(t)_r\right|^2} \quad (6b)$$

These two quantities provide the two dimensions of food security, which are how large and how stable food sufficiency is over time. The two quantities can also be thought of as two objectives to be optimized by adapting human agency under different climate and socioeconomic scenarios, e.g., in the form

$$\min(-\dot{\overline{\Psi}}_r, \sigma_{\overline{\Psi}_r}) \quad (7a, b)$$

Given the nature of the objective function being multi-objective, non-dominated sets of $(-\dot{\overline{\Psi}}_r, \sigma_{\overline{\Psi}_r})$ are sought. The human agency parameter tuples $[\tau_{L,r}, \tau_{MI,r}, \tau_{ML,r}]$ corresponding to non-dominated sets are identified as the adaptation by human agency to secure food. Non-

Table 1
Description of data used.

Data categories	Variables (symbol)	Unit	Period	Spatial Resolution	Temporal Resolution	Data source
Hydro-climatic	Temperature (T)	°C	2000–2017	0.5*0.5°	Daily time series distributed using monthly data	CRU (CRU, 1901–2017; Harris et al., 2014)
	Precipitation (P) For crop model calibration.	Mm	2000–2017	0.5*0.5°	Derived from monthly data. Growing-season-accumulated value for each year.	CRU (CRU1901-2017:Harris et al., 2014)
	Precipitation (P) For climate scenarios.		1969–2013	0.25*0.25°	Derived from daily data.	GLDAS Catchment Land Surface Model L4 daily 0.25*0.25° V2.0 (Li et al., 2018; Rodell et al., 2004)
	Transpiration (Tr)	W/m^2 (converted to mm)	2000–2017	0.25*0.25°	Derived from monthly data. Growing-season-accumulated value for each year.	GLDAS Noah Land Surface Model L4 monthly 0.25*0.25° V2.1 (Rodell et al., 2004)
Crop Information	NDVI (g)	–	2000–2017	30 m	Derived from 8-day data. Growing-season-maximum value for each year.	Landsat 7 NDVI (imported from Google Earth Engine: 'LANDSAT/LE07/C01/T1_8DAY_NDVI', Gorelick et al., 2017)
	Crop type & Growing season		1991–2010	Station-level	Yearly	National Meteorological Information Center of China (2006)
	Provincial crop yield (Y)	kg/ha	2001–2017	Provincial	Yearly	Statistical Yearbook of Jiangsu (BSJ, 2018)
	Crop plant area (A)	1000 ha (kha)	2001–2018	Provincial	Yearly	Statistical Yearbook of Jiangsu (BSJ, 2019)
	Crop cost per area (Y)	CNY/mu (1 mu = 1/15 ha)	2001–2018	Provincial	Yearly	China Rural Statistical Yearbook (NBS, 2016)
Human Agency	Total Population	10^4 Capita	2001–2019	Provincial	Yearly	Statistical Yearbook of Jiangsu (BSJ, 2019)
	Population Prediction Data 2011–2030	10^4 Capita	2011–2030			Compilation of population prediction data in Jiangsu Province 2011–2030 (BSJ, 2012)
	Population Prediction Data 2001–2050	10^4 Capita	2001–2050			Compilation of population prediction data in Jiangsu Province 2001–2050 (Bureau of Statistics of Jiangsu, 2002)
	Labor force in crop cultivation (L_C)	Capita/kha	2001–2017			Statistical Yearbook of Jiangsu (BSJ, 2018)
	Irrigation machinery (M_I)	Kw/kha				
	Land-preparing machinery (M_L)					
	Fertilizer use (F)	Ton/kha				

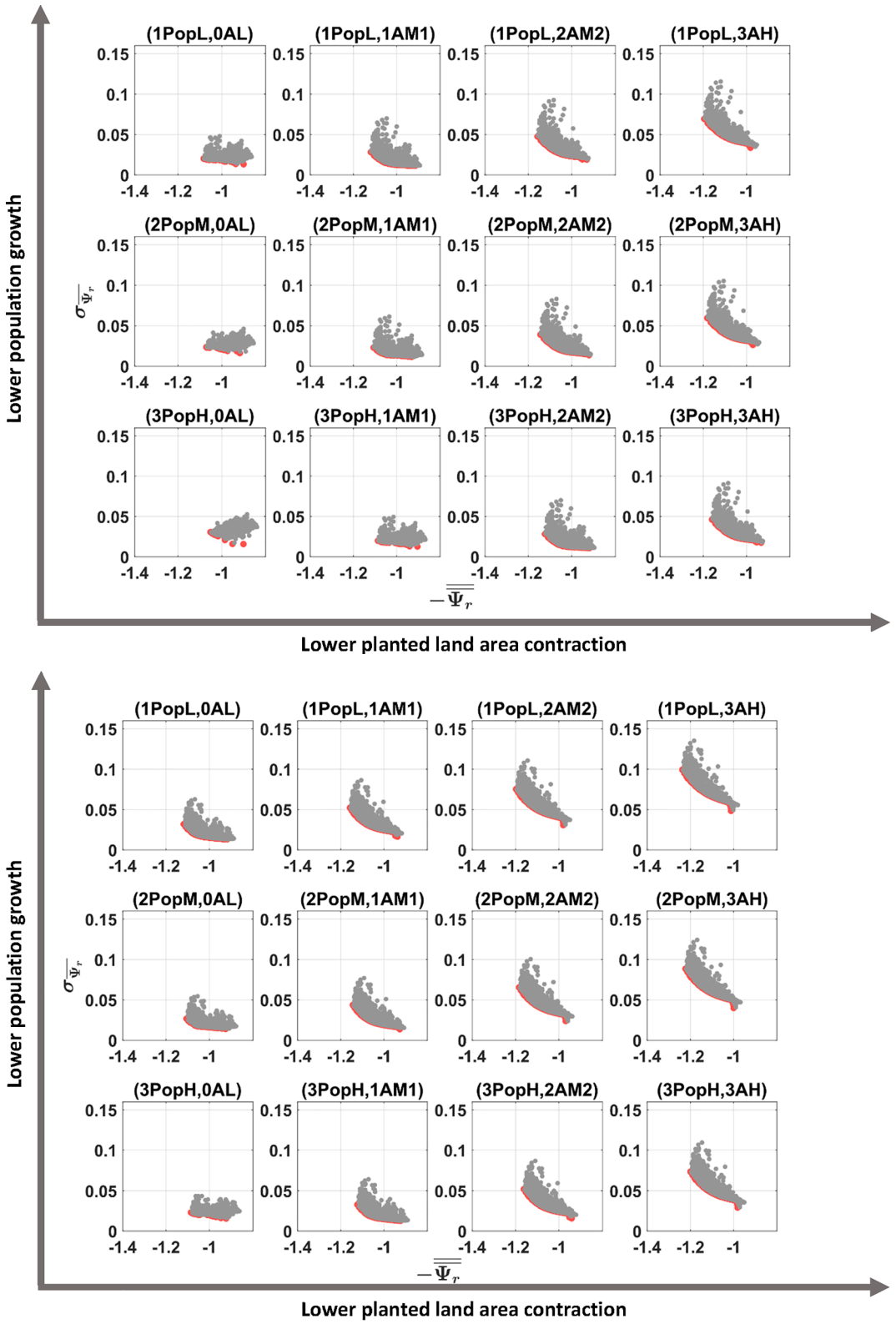

Fig. 7. a Food secure pareto frontiers under least optimistic climate scenario (RCP8.5, P10%). The x-axis shows the objective of minimizing the negative of average food self-sufficiency ratio ($-\dot{\overline{\Psi}}_r$), y-axis shows the objective of minimizing the standard deviation of self-sufficiency ratio over time, i.e., $\sigma_{\overline{\Psi}_r}$. Red markers represent the non-dominated sets of $(-\dot{\overline{\Psi}}_r, \sigma_{\overline{\Psi}_r})$, i.e., the food secure pareto frontier, while the grey markers represent the dominated set. b Food secure Pareto frontiers under most optimistic climate scenario (RCP2.6, P95%) Red markers represent the non-dominated sets of $(-\dot{\overline{\Psi}}_r, \sigma_{\overline{\Psi}_r})$, i.e., the food secure pareto frontier, while the grey markers represent the dominated set. (For interpretation of the references to color in this figure legend, the reader is referred to the web version of this article.)

Table 2
Population scenarios and its definitions in terms of fertility rate and time to peak (BSJ, 2002, 2012, 2019).

Year	Fertility rate (%)			Peak population (10^4)		
	Low (1PopL)	Mid (2PopM)	High (3PopH)	Low (1PopL)	Mid (2PopM)	High (3PopH)
2001~2019	Historical population data					
2020~2050	1.65	1.75	1.85	8139.8 (2024)	8167.5 (2025)	8241.1 (2026)

dominated sets are such that there are no other ways human agency can adapt that will result in both larger magnitude of food self-sufficiency ratio as well as stabler (i.e., with lower variance) ratio. These therefore describe how the time series of human agency should evolve over time in order to optimize food security for the region.

2.8. Data sources

The data sources of all the datasets are shown below in Table 1.

3. Results

3.1. Food secure non-dominated sets

Fig. 7a and b show the non-dominated sets (pareto frontier) of $(-\dot{\bar{\Psi}}_r, \sigma_{\bar{\Psi}_r})$ for two climate scenarios, which correspond to food secure options identified from amongst the simulated adaptation options by human agency (i.e., from 2000 random samples of tuples $[\tau_{L,r}, \tau_{MI,r}, \tau_{ML,r}]$).

The impact of crop plant area contraction scenarios on food security is most significant. Fig. 7a and b display the food security scenarios, including non-dominated sets, for the least optimistic climate scenario '(RCP8.5, P10%)' and the most optimistic climate scenario, '(RCP2.6, P95%)'. RCP 8.5 is generally taken as the basis for worst case climate change scenario, since it assumes that the emission of green-house gases will continue to rise throughout the 21st century. On the other hand, RCP 2.6 assumes the most stringent limitations on future green-house gas emissions. The temperature rise under RCP 8.5 is generally higher than that under RCP 2.6 as shown in Fig. 3a, b and leads to less precipitation.

In each of the figures, the three rows correspond to the three population scenarios named as '1PopL', '2PopM', '3PopH'. The definitions of these population scenarios are listed in Table 2.

The four columns of Fig. 7a and b correspond to the four crop planted area (A) scenarios, namely '0AL', '1AM1', '2AM2', and '3AH' (see Fig. 6). Here 'L' means low, standing for the most negative growth rate (i.e., contraction rates) of –33.93 kha/year after 2018 of planted area; M1 and M2 correspond to relatively mild planted area contraction rates after 2018, i.e. 75% and 50% of low scenario rates respectively. H means High, with a relatively stable growth rate of planted area after 2018, which is 25% of the value in the low scenario.

Both the figures confirm that the food secure (pareto) frontier moves towards higher level of average food sufficiency ratios when population growth rate is lower or planted area contracts slower. This is intuitive because faster population growth puts food security under stress, while more available land for crops leads to more production of food, thereby increasing food self-sufficiency.

Moreover, the pareto frontier rotates clockwise as higher levels of food self-sufficiency, $\dot{\bar{\Psi}}$, are achieved. This means that food self-sufficiency is more variable over time at higher levels of average food self-sufficiency, indicating that the tradeoff between the two objectives, i.e., min $-\dot{\bar{\Psi}}_r$ and min $\sigma_{\bar{\Psi}_r}$, increases with higher levels of average food self-sufficiency rate.

The pattern of the effects of climate scenarios on food self-sufficiency rate is similar to those of socio-economic scenarios. The food secure pareto frontier moves towards higher level of food sufficiency in the most optimistic scenario (RCP2.6, P95%), but with higher variability, than in the case of (RCP8.5, P10%).

3.2. Pareto optimal food self-sufficiency time series

Fig. 8a and b show the median values of average food self-sufficiency ratios for non-dominated human agency sets and for dominated sets (in gray) sets for the two scenarios (RCP8.5, P10%) and (RCP2.6, P95%). The time series are from 2018 to 2050, which are shown along with the historical values available from 2001 to 2017.

The (3PopH, 0AL) scenario is the worst socioeconomic scenario for food security for both the climate scenarios. The worst scenario is the least optimistic climate scenario with highest population growth rate and rapidly declining crop planted area. Under the scenario of rapidly declining crop planted area, the average food self-sufficiency rate drops below 1.0 when human agency doesn't adapt, indicating heightened risk of food insecurity. However, with adaptation by human agency, the food self-sufficiency rate is maintained above 1.0. This means that human agency has the ability to ensure food security even under least optimistic scenarios of the future.

Under the most optimistic socioeconomic scenario of (1PopL, 3AH) shown in Fig. 8b, the average food self-sufficiency rate keeps rising and finally reaches a value above 1.2. The most optimistic scenario is the most optimistic climate scenario with slowest growth in population and no contraction of available cropland. With food self-sufficiency rate higher than 1.0, the crop production within the province can satisfy the food demand of the province and outside. Also note that the difference between the dominated and non-dominated solutions is not as high as in the least optimistic scenario, meaning that adaptation by human agency plays a critical role when dealing with less optimistic future scenarios.

For the scenarios in between, average food self-sufficiency can be maintained between 1.0 and 1.2 when human agency adapts to changing conditions. Adaptation by human agency is important even under more optimistic scenarios since without it food self-sufficiency can fall below 1.0 (corresponding to the dominated food sufficiency time series). The median levels of food self-sufficiency for non-dominated solutions (red lines in Fig. 8a and b) are always higher than that of dominated solutions (gray line). Again, the gap between the non-dominated and the dominated time series is more significant under less optimistic scenarios, i.e., with higher temperature, less precipitation, less crop plant area, and more stress from population growth.

The subplot '3PopH, 0PAL' in Fig. 8a shows that the gap of food self-sufficiency between non-dominated and dominated solutions can exceed by 10% under the least optimistic climate and socioeconomic scenario. Under the scenarios of, e.g., lower pressure on cropland area and from population growth (from 0AL to 3AH), the gap between non-dominated and dominated solutions narrows and is between 5% and 10%. This indicates the importance of adaptation by human agency under more stressful climate and socioeconomic conditions, e.g., of drought, or fast-pace urbanization. Human agency, which is a combination of labor, irrigation and land-preparation machinery, can effectively ensure food security within Jiangsu Province under possible future water or land resources stresses.

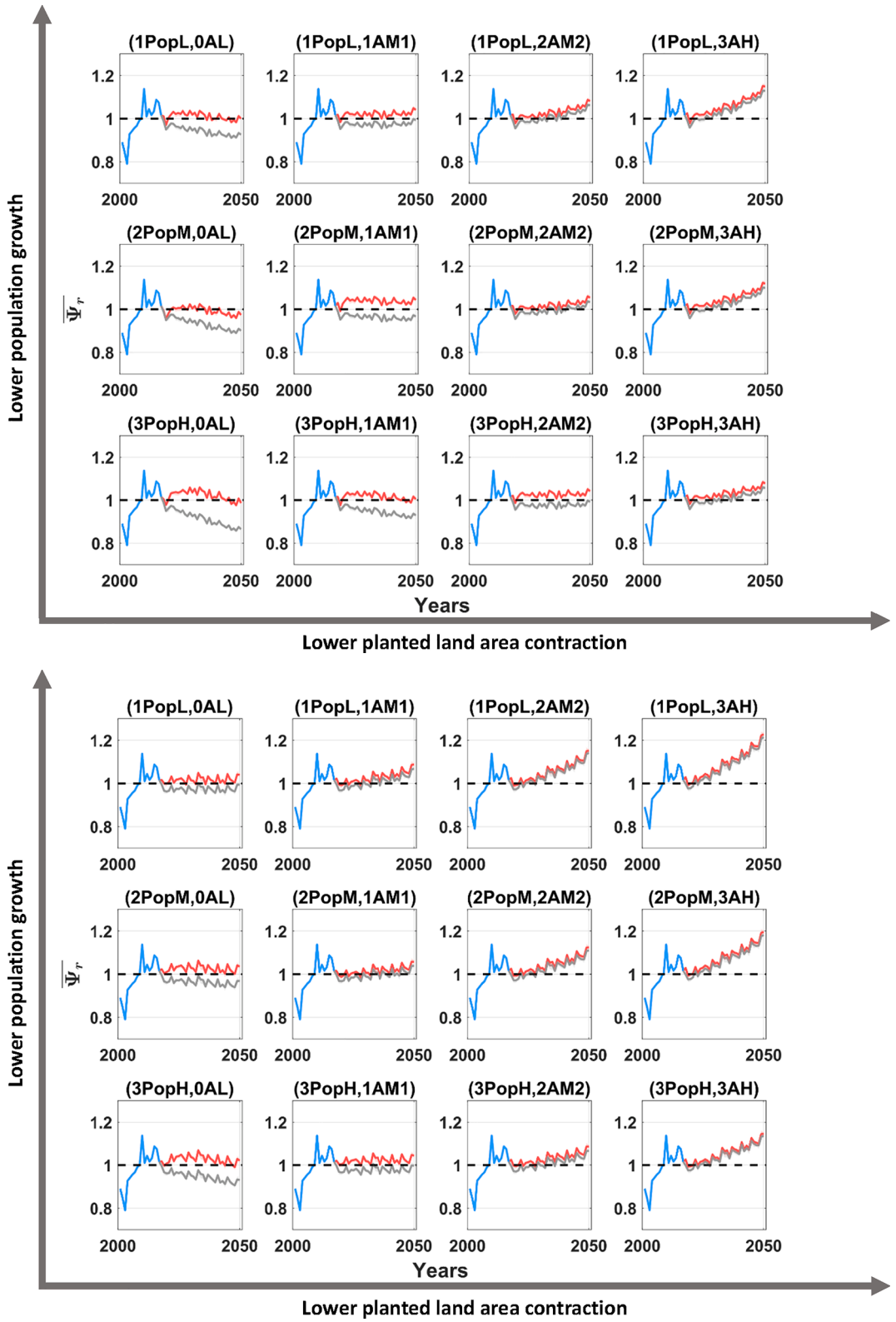

Fig. 8. a Median food self-sufficiency ratios time series $\overline{\Psi}(t)_r$ for dominated and non-dominated sets under climate scenario (RCP8.5 P10%). Blue line: historical time series; Red line: time series corresponding to non-dominated human agency sets; Grey line: time series corresponding to dominated sets. The province is self-sufficient if it remains above the dashed line (i.e., $\overline{\Psi}(t)_r > 1$). b Food self-sufficiency rate time series $\overline{\Psi}(t)_r$ for dominated and non-dominates sets for climate scenario (RCP2.6 P95%). Blue line: historical time series; Red line: optimized (non-dominated) time series; Grey line: dominated time series. The province is self-sufficient if it remains above the dashed line. (For interpretation of the references to color in this figure legend, the reader is referred to the web version of this article.)

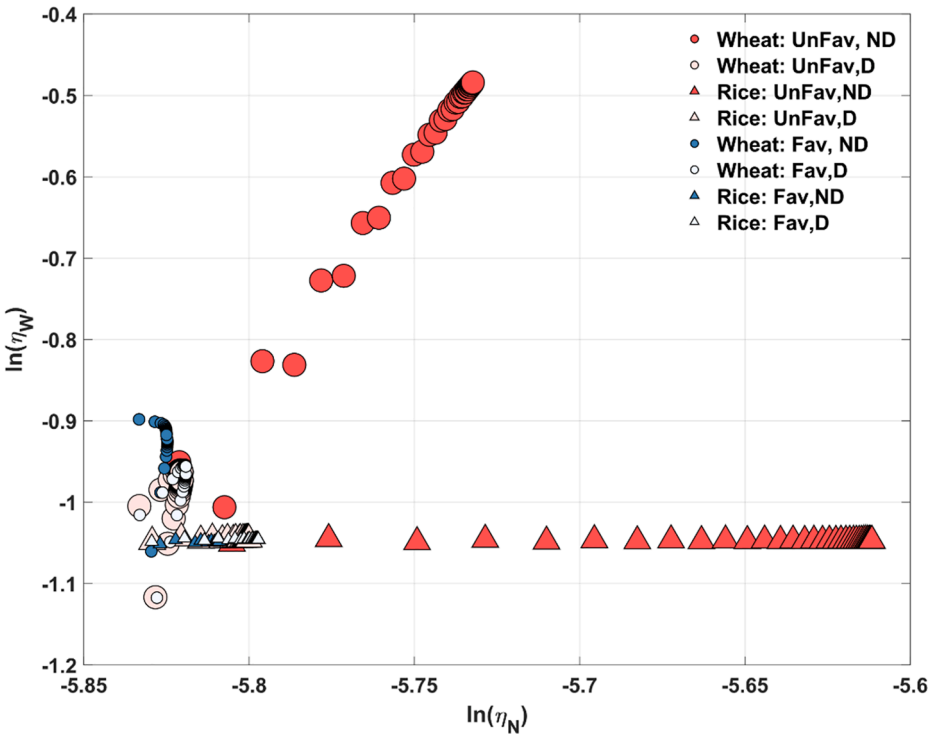

Fig. 9. Water and nutrient use efficiencies in log-space with optimized (non-dominated, ND) and dominated (D) solutions of human agency under unfavorable (UnFav) and favorable (Fav) scenarios. Unfavorable: least optimistic climate (RCP8.5, P10%), and most stressed socioeconomic scenario ('3PopH, 0AL') Favorable: most optimistic climate scenario (RCP2.6, P95%) and least stressed socioeconomic scenario ('1PopL, 3AH').

4. Discussion

4.1. Improving water and nutrient use efficiencies by adapting human agency

Modern technologies in agriculture such as irrigation and land preparation machineries can bring significant improvements in the water and nutrient use efficiencies of crops. Water-saving irrigation technology has been applied to 2637.47–2767.23 kha from 2017 to 2018 (Bureau of Statistics of Jiangsu, 2019), which is about 34.9–36.8% of total agricultural cropland within the province. Across China, latest technologies such as water-fertilizer integrated irrigation system based on Internet of Things (IoT) has also been designed and proposed (Shi et al., 2017; Hao et al., 2020). Also, land-preparing machinery are better in preparing croplands for higher nutrient use efficiency of food crops than human labor.

Fig. 9 shows the average level of water and nutrient use efficiencies in log-space under two extreme scenarios: most optimistic and least optimistic climate and socioeconomic scenarios.

The non-dominated efficiencies are higher in general under unfavorable conditions. More trade-off between the two in wheat production compared to rice is due to how sensitive crop specific efficiencies are related to human agency. The water use efficiency of wheat is sensitive to the human agency under non-dominated cases, while that of rice is not. However, the nutrient use efficiency of both wheat and rice can be significantly improved with adapting human agency, i.e. corresponding to non-dominated cases. The difference between non-dominated and dominated efficiencies under favorable conditions is insignificant, which again emphasizes that human agency matters when conditions are unfavorable. There is more scope for improving efficiencies when conditions are unfavorable due to poor water and land supply and high food demand.

4.2. Trade-offs between labor and machinery used

Fig. 10a and b plot labor (L_C) against land-preparing machinery power (M_L) for two climate scenarios: (RCP 8.5, P10%) and (RCP 2.6, P95%). The rows of each figure denote population growth rates (three levels from low to high), whereas the columns represent crop plant area contraction rates (four levels from low to high).

Modern machinery appears to be the main agency that delivers higher food self-sufficiency under all circumstances. Under unfavorable socioeconomic conditions, i.e., with higher population growth and sharper contraction of available land resources for crop cultivation, agricultural land-preparing machinery plays more important role to ensure nutrient and water use efficiency in order to increase the production of food crop, ensuring a higher and stabler supply of food. The effect of labor on food sufficiency is relatively low. This indicates that agricultural mechanization would ensure food security in Jiangsu Province under the unfavorable scenario of rapid urbanization. Agricultural lands will shrink in the process of urbanization. This will shift people from rural agriculture to modern industries, leading to rural to urban migration (Lyu et al., 2019). Agricultural mechanization can however replace the demand of shrinking human labor while ensuring same or higher levels of food production, thereby ensuring food security in the region.

Under the scenarios of less stressed socioeconomic conditions, i.e., lower population growth or lower contraction of crop planted area, the need for agricultural machinery, which can rapidly improve crop unit yields and thus result in higher food self-sufficiency rate, would not be that urgent compared to the unfavorable case. More labor can be hired to relieve under-employment in rural agriculture areas.

Similarly, in context of climate scenarios, agricultural labor demand would slightly rise in more optimistic climate scenarios since the urgency to use agricultural machinery is eased to a certain extent. When the climate is less optimistic, e.g. (RCP8.5, P10%), agricultural machinery is important agency that should be adapted to improve food crop production capacity and ensure high and stable food self-sufficiency.

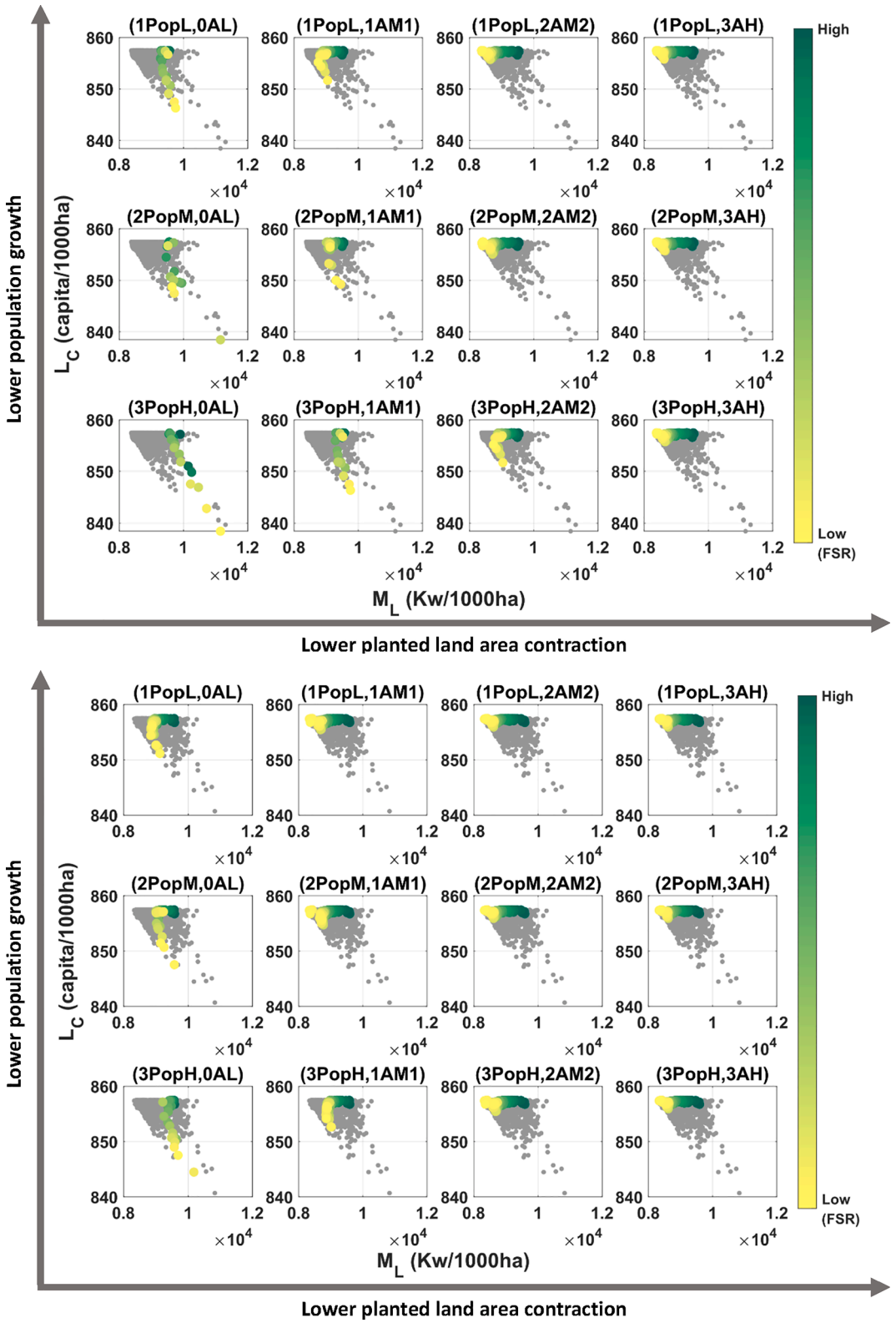

Fig. 10. a. Trade-off between crop labor force, L_C, and land-preparing machinery power, M_L, used under least optimistic climate scenario (RCP8.5, P10%). Points with color correspond to food secure pareto frontier Green color means higher average food self-sufficiency $\dot{\Psi}_r$, yellow color means lower $\dot{\Psi}_r$. b Trade-off between crop labor force L_C and land-preparing machinery power M_L under most optimistic climate scenario (RCP2.6, P95%) Points with color correspond to food secure pareto frontier Green color means higher food self-sufficiency rate $\dot{\Psi}_r$, yellow color means lower $\dot{\Psi}_r$. (For interpretation of the references to color in this figure legend, the reader is referred to the web version of this article.)

5. Conclusion

This study investigated how food security can be ensured within Jiangsu Province, China under different climate and socioeconomic scenarios by adapting human agency. The human agency comprises of crop production labor, irrigation machinery power and land-preparing machinery. Climate scenarios included six combinations of two RCPs (RCP 2.6, and RCP 8.5) and three percentiles (10%, 50%, 95%) of a distribution of GCMs most representative of the past climate conditions of the province. The socioeconomic scenarios considered combinations of three population growth rates and four rates of crop plant area growth into the future. Two crops, rice and wheat, were considered. The predicted time series of food self-sufficiency rate were evaluated, and trade-offs between human power and land-preparing machinery power were analyzed to reveal the critical role played by human agency in adapting to different climate and socio-economic conditions.

The results demonstrated that adapting human agency led to improved water and nutrient use efficiencies of crop production, especially in least optimistic climate and socioeconomic scenarios. The Jiangsu Province can be self-sufficient in food under all considered climate and socioeconomic scenarios considered when options are available for human agency to adapt. The gap between adaption and non-adaptation solutions was found to be larger under more challenging scenarios of lesser precipitation, higher population growth or stronger contraction of crop plant area. This suggests that human adaptation can significantly improve food security within Jiangsu Province especially when there are higher stresses of water or land resources insecurity.

Under lower water or land resources stress conditions, labor could replace land-preparing machinery since the level of food production can be easily maintained with abundant water and land availability. On the other hand, when climate change negatively affects the precipitation, or when population rises more rapidly, machinery such as water-saving irrigation or even water-fertilizer integrated irrigation systems together with land-preparing machinery, instead of human labor, could lead to higher levels of water and nutrient use efficiencies. These are much needed to secure food under adverse conditions.

The applied crop model (Lyu et al., 2020) ignores seeds and pesticides inputs to crop production. As reported in the literature, ignoring these inputs can lead to over-estimation of production levels (Zida et al., 2011). Similarly, only precipitation and temperature effects of climate change were considered and not those of CO2 fertilization. This may lead to under-estimation of production levels under adverse climate change scenarios (Rashid et al., 2019). We used historical 18 years agro-meteorological stations data. Here crop yields were not limited by availability of seeds and fertilizers, therefore it would not be possible to assess the effects of these inputs on crop yields and production. However, assessing the positive feedbacks between CO2 concentration and crop yields is possible. We defer this improvement in crop model for future research.

6. Declarations

The authors declare that there is no financial or personal interest or belief that could affect their objectivity.

CRediT authorship contribution statement

Haoyang Lyu: Conceptualization, Methodology, Software, Validation, Formal analysis, Investigation, Data curation, Writing - original draft, Writing - review & editing, Visualization. **Zengchuan Dong:** Supervision, Conceptualization. **Saket Pande:** Supervision, Conceptualization, Validation, Writing - review & editing.

Declaration of Competing Interest

The authors declare that they have no known competing financial interests or personal relationships that could have appeared to influence the work reported in this paper.

Appendix A. Supplementary data

Supplementary data to this article can be found online at https://doi.org/10.1016/j.jhydrol.2021.126344.

References

Achille, Jean, J., Folefack, 2015. The rural exodus of young farmers and its impact on the shortage of labor and food crop production in Cameroon: a computable general equilibrium model's analysis. J. Human Ecol. https://doi.org/10.1080/09709274.2015.11906838.

Aloysius, N.R., Sheffield, J., Saiers, J.E., Li, H., Wood, E.F., 2016. Evaluation of historical and future simulations of precipitation and temperature in central Africa from cmip5 climate models. J. Geophys. Res. Atmos. 121 (1), 130–152. https://doi.org/10.1002/2015JD023656.

Avery, S.V., Singleton, I., Magan, N., Goldman, G.H., 2019. The fungal threat to global food security. Fungal Biol. 123 (8), 555–557. https://doi.org/10.1016/j.funbio.2019.03.006.

Bureau of Statistics of Jiangsu (2018). Statistical Yearbook of Jiangsu: China Statistics Press. Retrieved from http://tj.jiangsu.gov.cn/col/col70123/index.html (Chinese version, access for free.).

Bureau of Statistics of Jiangsu. (2019). Statistical Yearbook of Jiangsu: China Statistics Press. Retrieved from http://tj.jiangsu.gov.cn/col/col70123/index.html (Chinese version, access for free.).

Bureau of Statistics of Jiangsu. (2002). Compilation of population prediction data in Jiangsu Province 2001-2050.

Bureau of Statistics of Jiangsu. (2012). Compilation of population prediction data in Jiangsu Province 2011-2030.

Cardwell, R., 2014. Food Security and International Trade. Springer, Netherlands.

Challinor, A.J., Simelton, E.S., Fraser, E.D., Hemming, D., Collins, M., 2010. Increased crop failure due to climate change: assessing adaptation options using models and socio-economic data for wheat in China. Environ. Res. Lett. 5 (3), 034012 https://doi.org/10.1088/1748-9326/5/3/034012.

Chen, Y., 2019. Path analysis of influencing factors of grain planting area from the perspective of supply side reform. J. Liaoning Univ. Technol. (Soc. Sci. Ed.) 21 (4), 36–39. https://doi.org/10.15916/j.issn1674-327x.2019.04.010.

Chen, Y., Zhou, H., Yin, G., 2016. Comparative analysis between the changes of corn planting area and the profitability in Northeast China from the perspective of planting substitutions. Res. Agric. Mod. 37 (3), 489–495. https://doi.org/10.13872/j.1000-0275.2016.0051.

Crane, T.A., Roncoli, C., Hoogenboom, G., 2011. Adaptation to climate change and climate variability: The importance of understanding agriculture as performance. NJAS-Wageningen J. Life Sci. 57 (3–4), 179–185. https://doi.org/10.1016/j.njas.2010.11.002.

Eyring, V. (2013). Performance metrics and observations in global climate model evaluation. ESA CMUG Integration-3 meeting. DLR.

Febrina Torop Simangunsong, Sumono Sumono, Ainun Rohana, Edi Susanto. (2013). Drip irrigation efficiency analysis and crop water requirements of mustard (brassica juncea) in the inceptisol soil. Jurnal Rekayasa Pangan Dan Pertanian.

Garibaldi, L.A., Pérez-Méndez, N., 2019. Positive outcomes between crop diversity and agricultural employment worldwide. Ecol. Econ. 164, 106358 https://doi.org/10.1016/j.ecolecon.2019.106358.

Gomez-Zavaglia, A., Mejuto, J.C., Simal-Gandara, J., 2020. Mitigation of emerging implications of climate change on food production systems. Food Res. Int. 109256 https://doi.org/10.1016/j.foodres.2020.109256.

Gorelick, N., Hancher, M., Dixon, M., Ilyushchenko, S., Thau, D., Moore, R., 2017. Google earth engine: planetary-scale geospatial analysis for everyone. Remote Sens. Environ. 202, 18–27. https://doi.org/10.1016/j.rse.2017.06.031.

Greene, A.M., Hellmuth, M., Lumsden, T., 2012. Stochastic decadal climate simulations for the Berg and Breede water management areas, western Cape province, South Africa. Water Resour. Res. 48 (6) https://doi.org/10.1029/2011WR011152.

Greene, A.M., 2012. The simgen Software Package: User Guide and Notes. International Research Institute for Climate and Society.

Greene, A.M., Goddard, L., Gonzalez, P.L., Ines, A.V., Chryssanthacopoulos, J., 2015. A climate generator for agricultural planning in southeastern South America. Agric. For. Meteorol. 203, 217–228. https://doi.org/10.1016/j.agrformet.2015.01.008.

Gu, L., & Guo, Q. (2011). Evolution and development of China's major grain producing areas. Issues Agri. Econ., 2011(8), 4-9. Doi: CNKI:SUN:NJWT.0.2011-08-001.

Hao, Y., Hu, X., Li, F., 2020. Water and fertilizer integrated irrigation system based on Internet of Things technology. Internet Things Technol. 9, 58–61. https://doi.org/10.16667/j.issn.2095-1302.2020.09.017.

Harris, I. P. D. J., Jones, P. D., Osborn, T. J., & Lister, D. H. (2014). Updated high-resolution grids of monthly climatic observations–the CRU TS3. 10 Dataset. Int. J. Climatol., 34(3), 623-642. Doi: 10.1002/joc.3711.

Hertel, T.W., Rosch, S.D., 2010. Climate change, agriculture and poverty. The World Bank. https://doi.org/10.1596/1813-9450-5468.

Hibbard, K.A., Meehl, G.A., Cox, P.M., Friedlingstein, P., 2007. A strategy for climate change stabilization experiments. Eos, Trans. Am. Geophys. Union 88 (20), 217–221. https://doi.org/10.1029/2007EO200002.

Hou, H., Wang, R., Murayama, Y., 2019. Scenario-based modelling for urban sustainability focusing on changes in cropland under rapid urbanization: a case study of Hangzhou from 1990 to 2035. Sci. Total Environ. 661, 422–431. https://doi.org/10.1016/j.scitotenv.2019.01.208.

Huang, M., Wang, Z., Luo, L., Wang, S., Cao, H., He, G., & Diao, C. (2018). Effects of ridge mulching, furrow seeding, and optimized fertilizer placement on NPK uptake and utilization in dryland wheat. J. Plant Nutri. Fertilizers. 2018, 24(5): 1158–1168. Doi: 10.11674/zwyf.17463.

Hurrell, J., Visbeck, M., Pirani, P., 2011. WCRP coupled model intercomparison project-phase 5-CMIP5. Clivar Exchanges 16 (56).

Kaiser, M.L., 2011. Food security: an ecological–social analysis to promote social development. J. Community Practice 19 (1), 62–79. https://doi.org/10.1080/10705422.2011.550261.

Kakinuma, K., Yoshikawa, S., Endo, T., Kanae, S. (2014). Water law as an adaptation strategy for global water scarcity in the future. Agu Fall Meeting. AGU Fall Meeting Abstracts. Retrieved from: https://ui.adsabs.harvard.edu/abs/2014AGUFM.H13A1039K/abstract.

Kawuma Menya, C. (2011). Rainfall variation due to climate change: an intertemporal investigation into its impact on susbsistence crop net revenue. URI: http://hdl.handle.net/11250/187225.

Kotu, V., Deshpande, B., 2018. Data Science: Concepts and Practice. Morgan Kaufmann.

Kukal, M.S., Irmak, S., 2018. Climate-driven crop yield and yield variability and climate change impacts on the US Great Plains agricultural production. Sci. Rep. 8 (1), 1–18. https://doi.org/10.1038/s41598-018-21848-2.

Leisnham, P. T., Montas, H., Shirmohammadi, A., Chanse, V., Lansing, D., Rockler, A., et a. (2013). Watershed diagnostics for improved adoption of management practices: Integrating biophysical and social factors across urban and agricultural landscapes. In 2013 Kansas City, Missouri, July 21-July 24, 2013 (p. 1). American Society of Agricultural and Biological Engineers. Doi: https://doi.org/10.13031/aim.20131668614.

Li, Bailing, H. Beaudoing, and M. Rodell, NASA/GSFC/HSL (2018), GLDAS Catchment Land Surface Model L4 daily 0.25 x 0.25 degree V2.0, Greenbelt, Maryland, USA, Goddard Earth Sciences Data and Information Services Center (GES DISC), Accessed: [1969.1.1 - 2013.12.31], 10.5067/LYHA9088MFWQ.

Li, B., & Sivapalan, M. (2020). Long-term coevolution of an urban human-water system under climate change: critical role of human adaptive actions. Water Resour. Res., 55, e2020WR027931. Doi: 10.1029/2020WR027931.

Li, G., X, J., & Li, F. (2009). Analysis of the restriction factors and approaches to increase grain production in Jiangsu Province. J. Nanjing Univ. Finance Econ., 2009 (3), 20-24.

Li, J., Li, L., 2012. Water resources supporting capacity to regional socio-economic development of China. Acta Geographica Sinica 67 (3), 410–419. https://doi.org/10.11821/xb201203012.

Lobell, D.B., Field, C.B., Cahill, K.N., Bonfils, C., 2006. Impacts of future climate change on California perennial crop yields: Model projections with climate and crop uncertainties. Agric. For. Meteorol. 141 (2–4), 208–218. https://doi.org/10.1016/j.agrformet.2006.10.006.

Lyu, H., Dong, Z., Roobavannan, M., Kandasamy, J., Pande, S., 2019. Rural unemployment pushes migrants to urban areas in Jiangsu Province, China. Palgrave Commun. 5 (1), 1–12. https://doi.org/10.1057/s41599-019-0302-1.

Lyu, H., Dong, Z., Pande, S., 2020. Interlinkages between human agency, water use efficiency and sustainable food production. J. Hydrol. 582, 124524 https://doi.org/10.1016/j.jhydrol.2019.124524.

Ma, X., Sanguinet, K.A., Jacoby, P.W., 2020. Direct root-zone irrigation outperforms surface drip irrigation for grape yield and crop water use efficiency while restricting root growth. Agric. Water Manag. 231, 1–11. https://doi.org/10.1016/j.agwat.2019.105993.

Makowski, D., Marajo-Petitzon, E., Durand, J.L., Ben-Ari, T., 2020. Quantitative synthesis of temperature, CO2, rainfall, and adaptation effects on global crop yields. Eur. J. Agron. 115, 126041 https://doi.org/10.1016/j.eja.2020.126041.

McCarthy, U., Uysal, I., Badia-Melis, R., Mercier, S., O'Donnell, C., Ktenioudaki, A., 2018. Global food security–Issues, challenges and technological solutions. Trends Food Sci. Technol. 77, 11–20. https://doi.org/10.1016/j.tifs.2018.05.002.

Meehl, G.A., Hibbard, K.A., 2007. A strategy for climate change stabilization experiments with AOGCMs and ESMs. WCRP Informal Rep. 3, 2007.

Mo, F., Wang, G., Hu, M., 2020. Analysis of soybean production status in Northeast China based on cost. Soybean Sci. 39 (6), 947–953. https://doi.org/10.11861/j.issn.1000-9841.2020.06.0947.

Mondal, M., Sanaul, H., 2019. The implications of population growth and climate change on sustainable development in Bangladesh. Jàmbá: J. Disaster Risk Stud. 11 (1), 1–10. https://doi.org/10.4102/jamba.v11i1.535.

National Bureau of Statistics of China. (2016). China Rural Statistical Yearbook: China Statistics Press. Retrieved from https://navi.cnki.net/KNavi/YearbookDetail?pcode=CYFD&pykm=YMCTJ&bh=.

National Meteorological Information Center of China, Crop growth and development and farmland soil moisture data set in China. 2006.

Olesen, J.E., Trnka, M., Kersebaum, K.C., Skjelvåg, A.O., Seguin, B., Peltonen-Sainio, P., Micale, F., 2011. Impacts and adaptation of European crop production systems to climate change. Eur. J. Agron. 34 (2), 96–112. https://doi.org/10.1016/j.eja.2010.11.003.

Preston, B.L., King, A.W., Ernst, K.M., Absar, S.M., Nair, S.S., Parish, E.S., 2015. Scale and the representation of human agency in the modeling of agroecosystems. Curr. Opin. Environ. Sustain. 14, 239–249. https://doi.org/10.1016/j.cosust.2015.05.010.

Qian, Xiaolong, Guan, Hua, & Yuan, Xiaoyan. (2008). Empirical study on utilization benefit of cultivated land in Jiangsu Province. System Sci. Comprehensive Stud. Agri., 24 (2), 163-166,171. Doi: 10.3969/j.issn.1001-0068.2008.02.008.

Qiu, B., Li, H., Tang, Z., Chen, C., Berry, J., 2020. How cropland losses shaped by unbalanced urbanization process? Land Use Policy 96, 104715. https://doi.org/10.1016/j.landusepol.2020.104715.

Rashid, M.A., Jabloun, M., Andersen, M.N., Zhang, X., Olesen, J.E., 2019. Climate change is expected to increase yield and water use efficiency of wheat in the north china plain. Agric. Water Manag. 222, 193–203. https://doi.org/10.1016/j.agwat.2019.06.004.

Rodell, M., Houser, P.R., Jambor, U., Gottschalck, J., Mitchell, K., Meng, C., Arsenault, K., Cosgrove, B., Radakovich, J., Bosilovich, M., Entin, J.K., Walker, J.P., Lohmann, D., Toll, D., 2004. The global land data assimilation system. Bull. Amer. Meteor. Soc. 85, 381–394. https://doi.org/10.1175/BAMS-85-3-381.

Rosemberg, A., 2010. Building a just transition: the linkages between climate change and employment. Retrieved from: Int. J. Labour Res. 2 (2), 125 Https://search.proquest.com/docview/884976739/fulltext/8F5C77FD512543F9PQ/1?accountid=27026.

Schmidhuber, J., Tubiello, F.N., 2007. Global food security under climate change. Proc. Natl. Acad. Sci. 104 (50), 19703–19708. https://doi.org/10.1073/pnas.0701976104.

Shi, Z., Liu, Q., Bai, M., Shi, Y., Zhang, S., 2017. Water and fertilization integrated intelligent irrigation system design and benefit analysis based on the Internet of Things. J. Water Resour. Water Eng. 28 (3), 221–227. https://doi.org/10.11705/j.issn.1672-643X.2017.03.40.

Siwar, C., Ahmed, F., Begum, R.A., 2013. Climate change, agriculture and food security issues: Malaysian perspective. J. Food Agric. Environ. 11 (2), 1118–1123.

Springmann, M., Mason-D'Croz, D., Robinson, S., Garnett, T., Godfray, H.C.J., Gollin, D., Scarborough, P., 2016. Global and regional health effects of future food production under climate change: a modelling study. Lancet 387 (10031), 1937–1946. https://doi.org/10.1016/S0140-6736(15)01156-3.

Taylor, K.E., Stouffer, R.J., Meehl, G.A., 2012. An overview of CMIP5 and the experiment design. Bull. Am. Meteorol. Soc. 93 (4), 485–498. https://doi.org/10.1175/BAMS-D-11-00094.1.

Turral, H., Burke, J., & Faurès, J. M. (2011). Climate change, water and food security (No. 36). Food and Agriculture Organization of the United Nations (FAO). Retrieved from: http://www.fao.org/3/i2096e/i2096e00.htm.

van Vliet, J., Eitelberg, D.A., Verburg, P.H., 2017. A global analysis of land take in cropland areas and production displacement from urbanization. Global Environ. Change 43, 107–115. https://doi.org/10.1016/j.gloenvcha.2017.02.001.

Wang, H., Guo, F., Li, X. (2013) China Grain Map: From "South-to-North Grain Transport" to "North-to-South Grain Transport", 2013(25). Retrieved from: http://www.ceweekly.cn/2013/0701/32114.shtml.

Wang, Y.S., 2019. The challenges and strategies of food security under rapid urbanization in China. Sustainability 11 (2), 542. https://doi.org/10.3390/su11020542.

Warner, K., Van der Geest, K., 2013. Loss and damage from climate change: local-level evidence from nine vulnerable countries. Int. J. Global Warm. 5 (4), 367–386.

Xu, J., Ding, Y., 2015. Research on early warning of food security using a system dynamics model: evidence from Jiangsu province in China. J. Food Sci. 80 (1), R1–R9. https://doi.org/10.1111/1750-3841.12649.

Xu, L., Huang, Y., Liu, A., 2011. Study on the carrying capacity of water resources in Jiangsu Province based on the principal component analysis. Resour. Environ. Yangtze Basin 20 (12), 1468–1474.

Zhang, Yueping, Liu, youzhao, Mao, Liangxiang, Zhang, bingning. (2004). Evaluation of the security of land resources by land carrying capacity——a case study of Jiangsu Province. Resour. Environ. Yangtze Basin, 13 (4), 328-332. Doi: 10.3969/j.issn.1004-8227.2004.04.006.

Zhao, Y., Yan, W., 2019. Can China's grain acreage respond correctly to market mechanism? An empirical study based on panel simultaneous equations. J. Agro-Forestry Econ. Manage. 18 (3), 313–324. https://doi.org/10.16195/j.cnki.cn36-1328/f.2019.03.35.

Zhu, J., Ou, X., 2020. Research on the allometric growth and coordinated development of population land urbanization in Jiangsu. Territory Nat. Resour. Study 185 (2), 37–42. https://doi.org/10.16202/j.cnki.tnrs.2020.02.010.

Zida, E.P., Lund, O.S., Néya, J.B., 2011. Seed treatment with a binary pesticide and aqueous extract of eclipta alba (l.) hassk. for improving sorghum yield in burkina faso. J. Trop. Agric. 50, 1–7.